JOURNAL OF AGRICULTURAL AND FOOD CHEMISTRY

Article

pubs.acs.org/JAFC

p-Terphenyl Derivatives from the Mushroom *Thelephora aurantiotincta* Suppress the Proliferation of Human Hepatocellular Carcinoma Cells via Iron Chelation

Toshio Norikura,*[,†] Kenshu Fujiwara,[‡] Takanori Yanai,[§] Yusuke Sano,[‡] Takuto Sato,[‡] Takayuki Tsunoda,[‡] Keisuke Kushibe,[‡] Akiko Todate,[#] Yae Morinaga,[†] Kunihisa Iwai,[†] and Hajime Matsue[†]

[†]Department of Nutrition, Faculty of Health Science, Aomori University of Health and Welfare, Mase 58-1, Hamadate, Aomori 030-8505, Japan

[‡]Department of Chemistry, Faculty of Science, Hokkaido University, Sapporo 060-0810, Japan

[§]Department of Radiobiology, Institute for Environmental Sciences, Hacchazawa 2-121, Takahoko, Rokkasho, Aomori 039-3213, Japan

[#]JAC Company, Ltd., Higashiyama 1-2-7, Meguro-Ku, Tokyo 153-0043, Japan

Supporting Information

ABSTRACT: A novel 2′,3′-dihydroxy-*p*-terphenyl derivative, thelephantin O (TO), which has cancer-selective cytotoxicity, was isolated. This study investigated the underlying basis of the cytotoxicity of 2′,3′-dihydroxy-*p*-terphenyl compounds in view of their ability to chelate metal ions. $FeCl_2$ significantly reduced TO-induced cytotoxicity, whereas several other salts of transition metals and alkaline-earth metals did not. A structure−activity relationship study using newly synthesized *p*-terphenyl derivatives revealed that *o*-dihydroxy substitution of the central benzene ring was necessary for both the cytotoxicity and Fe^{2+} chelation of the compounds. Real-time PCR array and cell cycle analysis revealed that the TO-induced cytotoxicity was attributed to cell cycle arrest at the G1 phase via well-known cell cycle-mediated genes. The TO-induced changes in the cell cycle and gene expression were completely reversed by the addition of $FeCl_2$. Thus, it was concluded that Fe^{2+} chelation occurs upstream in the pivotal pathway of 2′,3′-dihydroxy-*p*-terphenyl-induced inhibition of cancer cell proliferation.

KEYWORDS: *2′,3′-dihydroxy-p-terphenyl derivatives, Thelephora aurantiotincta, thelephantin O, structure−activity relationships, cytotoxicity, Fe^{2+} chelation*

INTRODUCTION

Natural products are excellent sources of lead compounds to develop new drugs for the treatment of diseases. This is particularly evident in the treatment of cancers, in which more than 60% of drugs are of natural origin.[1] Hence, newly identified natural compounds with anticancer activity could represent a new tool for cancer therapy.

Mushrooms belonging to the genus *Thelephora*, which are widely distributed in East Asia, Australia, and America, are rich sources of biologically active compounds. Previous phytochemical investigations conducted on the genus *Thelephora* revealed that this genus is an abundant source of *p*-terphenyl derivatives.[2] *Thelephora aurantiotincta*, which belongs to this genus and grows in symbiosis with pine trees, is sold in a mixture with *Thelephora ganbajun* as an edible mushroom, the unique flavor and taste of which are appreciated in the Yunnan province of China.[3] During screening for bioactive compounds from *T. aurantiotincta*, we isolated a novel 2′,3′-dihydroxy-*p*-terphenyl derivative, thelephantin O (TO), and a known compound, vialinin A (VA), as selective cytotoxic agents against cancer cells (Figure 1).[4]

A previous study has shown that VA showed strong DPPH free radical scavenging activity[5] and inhibited tumor necrosis factor α production in activated mast cells and basophils[6] and, thus, was considered a promising candidate for a new type of antiallergic agent. To identify the target molecule of VA and develop a new antiallergic drug, VA and its structural derivatives, that is, atromentin, ganbajunin D, ganbajunin E, and thelephantin G, have been chemically synthesized, and their structure−activity relationships have been published.[7,8] These studies suggested that positional isomers of VA showed no such bioactivities and that no correlation existed between free radical scavenging activity and antiallergic activity. However, the active sites of these *p*-terphenyl derivatives have yet to be fully clarified.

We have recently reported the chemical synthesis of TO, VA, and other 2′,3′-dihydroxy-*p*-terphenyl derivatives such as terrestrins B−D via a practical route and the presence of cytotoxicity against cancer cells in the synthetic compounds.[9] However, the underlying basis of the cytotoxicity of 2′,3′-dihydroxy-*p*-terphenyl compounds remains to be elucidated. Therefore, the aims of this study were as follows: (i) to identify the active sites of the 2′,3′-dihydroxy-*p*-terphenyl derivatives for their bioactivity, that is, cytotoxicity against HepG2 cells and DPPH free radical scavenging activities, and (ii) to clarify the

Received: September 24, 2012
Revised: January 7, 2013
Accepted: January 22, 2013
Published: January 22, 2013

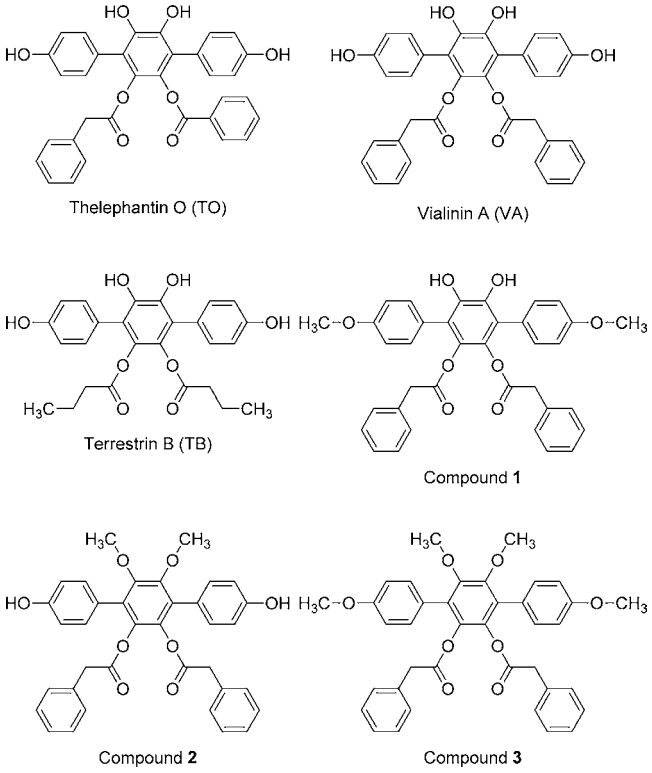

Figure 1. Structures of *p*-terphenyl derivatives.

mechanistic details for the cytotoxicity of the 2′,3′-dihydoroxy-*p*-terphenyl derivatives against HepG2 cells.

In this study, we designed and synthesized three new *p*-terphenyl analogues (compounds **1**−**3**), which had a VA skeleton bearing partially or fully protected hydroxyl groups, to obtain structural information on the biological activities of the 2′,3′-dihydroxy-*p*-terphenyl derivatives at the molecular level. Cytotoxicity against a human hepatocellular carcinoma cells line (HepG2) and DPPH free radical scavenging activity of these *p*-terphenyl derivatives, TO, VA, terrestrin B (TB), and compounds **1**−**3** were first examined. The structure−activity relationship study revealed that the *o*-dihydroxy substitution of the central benzene ring of the *p*-terphenyl derivatives was necessary for the cytotoxicity against HepG2 cells and DPPH free radical scavenging activity. By analogy with naturally occurring polyphenols, which were reported to have radical stabilizing and metal chelating functions in the *o*-dihydroxy benzene structure,[10] it was expected that the 2′,3′-dihydroxy-*p*-terphenyl derivatives would have the same functions. In addition, cancer cells are known to require larger amounts of metal ions, such as iron, copper, and zinc ions, for growth and proliferation than normal cells.[11] Therefore, we hypothesize that the cancer-selective cytotoxicity of 2′,3′-dihydroxy-*p*-terphenyl derivatives TO and VA would result from metal chelation, which would reduce the concentration of metal ions in cancer cells. To verify this hypothesis, we examined the participation of metal ions in TO-induced cytotoxicity against HepG2 cells to ascertain the participation of Fe^{2+}, which was supported by confirming the chelating ability of the 2′,3′-dihydroxy-*p*-terphenyl derivatives for Fe^{2+}.

MATERIALS AND METHODS

Materials. Dulbecco's modified Eagle's medium (DMEM) and phosphate-buffered saline (PBS) were purchased from Nissui Pharmaceutical (Tokyo, Japan). Fetal bovine serum (FBS) was purchased from BioWest (Nuaillé, France). TO, VA, and terrestrin B (TB) were prepared by chemical synthesis according to the method that we have recently reported.[9] The synthetic compounds **1**−**3** were prepared according to the procedure described in the Supporting Information.

DPPH Free Radical Scavenging Activity. The free radical scavenging activity of *p*-terphenyl derivatives was evaluated using DPPH according to a previously reported method.[12] Briefly, various concentrations of ethanol solutions of *p*-terphenyl derivatives (2 mL) were mixed with 0.5 mM DPPH ethanol solution (1 mL) and 0.1 M acetate buffer (pH 5.5; 2.0 mL). After 30 min of standing, the absorbance of the mixture was measured at 517 nm. DPPH solution without *p*-terphenyl derivatives was used as control, and 40% ethanol was used as blank. The relative DPPH free radical scavenging activity (%) was calculated as follows: [1 − (absorbance of sample)/(absorbance of control)] × 100.

Cell Culture. HepG2 cells were provided by the Riken Cell Bank (Tsukuba, Japan). HepG2 cells were maintained in ⌀ 100 mm dishes (Iwaki Glass, Tokyo, Japan) in DMEM containing 10% FBS, 100 U/mL penicillin, and 100 ng/mL streptomycin (Invitrogen Corp., Carlsbad, CA, USA) at 37 °C in an atmosphere of 5% CO_2 before use. For the experiments, the cells were seeded at a concentration of 4×10^5 cells/⌀ 35 mm dish and precultured for 1 day. Cells were synchronized at the G0/G1 phase of the cell cycle by serum starvation. Briefly, cells were cultured in serum-free medium for 36 h. At the time point "0 h," the medium was changed to 10% FBS containing DMEM with or without TO and a transition or alkaline-earth metal salts ($CuCl_2$, $FeCl_2$, $MgCl_2$, $MnCl_2$, or $ZnCl_2$). For the main culture, TO was dissolved in DMSO and diluted in culture medium immediately before use (final DMSO concentration, 0.25%).

Cell Viability Assay. Cell viability was measured by performing the Neutral Red assay, as described previously,[13] with minor modifications. This value indicates the cytotoxic and/or antiproliferative activities against HepG2 cells. A Neutral Red stock solution (0.4% Neutral Red in water) was diluted 1:80 (v/v) in PBS. After the main culture (48 h), the cells were incubated with Neutral Red solution for 30 min at 37 °C to allow the lysosomes of the viable cells to take up the dye. The Neutral Red solution was removed, a mixture of 1% acetic acid and 50% ethanol was added to the cells to extract the Neutral Red from viable cells, and the mixture was left at room temperature for 30 min. The absorbance of each sample was measured at 540 nm with a microplate reader. The relative cell viability (%) for the control wells containing the cell culture medium without samples was calculated as follows: [(absorbance of sample)/(absorbance of control)] × 100.

Cell Cycle Assay. After the main culture (6−18 h), cells were harvested by trypsinization, washed with PBS, and fixed with 70% (v/v) ethanol overnight at −20 °C. The fixed cells were incubated with freshly prepared RNase solution (200 μg/mL in PBS) for 30 min at 37 °C and then stained with propidium iodide solution (200 μg/mL in PBS) on ice for 30 min. The propidium iodide−DNA complex in each cell nucleus was measured by flow cytometry using FACSAria (BD Biosciences, Franklin Lakes, NJ, USA).

Real-Time RT-PCR Array. After the main culture (12 h), cells were washed twice with PBS, and total RNA was isolated from HepG2 cells by using a SV total RNA preparation kit (Promega, Madison, WI, USA), according to the manufacturer's instructions. The cDNA for each microgram of total RNA was obtained using the RT2 First Strand kit (Qiagen, Tokyo, Japan) according to the manufacturer's instructions. Briefly, after genomic DNA was removed, reverse transcription was performed at 42 °C for 15 min, after which the mixture was heated at 95 °C for 5 min to inactivate the enzyme. The cDNA was mixed with RT2 SYBR green/ROX qPCR master mix (Qiagen), and aliquots were loaded into each well of the RT2 Profiler PCR Array PAHS-020A (Qiagen). The PCR array was designed to study the profile of 84 human cell cycle-related genes. PCR array experiments were performed on an ABI 7000 instrument (Applied Biosystems, Foster City, CA, USA). Conditions for amplification were as follows: 2 cycles of 10 min at 95 °C, followed by 40 cycles of 15 s at 95 °C, and 1 min at 60 °C. The PCR array data were analyzed by the ΔΔCt method. The average of three

housekeeping genes (*B2M*, *HPRT1*, and *GAPDH*) was used to obtain the ΔCt for each gene of interest. The ΔΔCt value for each gene was calculated by the difference between the ΔCt of the treated and the ΔCt of the control groups. The fold change for each gene was calculated by $2^{-\Delta\Delta Ct}$ using RT2 Profiler PCR Array Data Analysis Web-based software (Qiagen).

Iron Chelating Activity. Iron (Fe^{2+}) chelation activity of *p*-terphenyl derivatives was estimated as previously described,[14] with minor modifications. Briefly, 1.6 mM $FeSO_4$ solution and 1 mM ferrozine solution were prepared and diluted (5 times) with assay buffer (130 mM NaCl, 10 mM KCl, 1 mM $MgSO_4$, 5 mM glucose, and 50 mM HEPES, pH 7.0) at the time of the experiment. Next, 750 μL of diluted ferrozine and 800 μL of the *p*-terphenyl derivatives (in methanol) were mixed, and the reaction was initiated by the addition of 50 μL of diluted $FeSO_4$. The solutions were mixed well and allowed to stand for 20 min. After incubation, the absorbance was measured at 562 nm. The percentage of the iron chelating effect was calculated as follows: iron chelating activity (%) = [1 − (absorbance of sample)/(absorbance of control)] × 100.

Statistical Analysis. Data are expressed as the mean ± SD values of three or four independent experiments. Statistical differences in assay values were evaluated with a one-way ANOVA, followed by Dunnett's multiple-comparison post hoc test. Statistical analysis (Figures 2−4) was performed with KyPlot version 4.0 (KyensLab Inc., Tokyo, Japan). Statistical analyses of the PCR array, carried out to determine differences between the treatment and control groups, were performed using RT2 Profiler PCR Array Data Analysis Web-based software (Qiagen). For all statistical analyses, a *p* value of <0.01 was considered to be significant.

RESULTS

Cytotoxicity against HepG2 Cells and DPPH Free Radical Scavenging Activity of *p*-Terphenyl Derivatives. The cytotoxicity against HepG2 cells and DPPH free radical scavenging activity of six *p*-terphenyl derivatives (Figure 1) were evaluated. As shown in Figure 2A, TO, VA, TB, and compound **1** showed almost similar cytotoxicities, which followed a dose-dependent pattern; however, compounds **2** and **3** did not. Similarly, TO, VA, TB, and compound **1**, but not compounds **2** and **3**, showed DPPH free radical scavenging activity (Figure 2B).

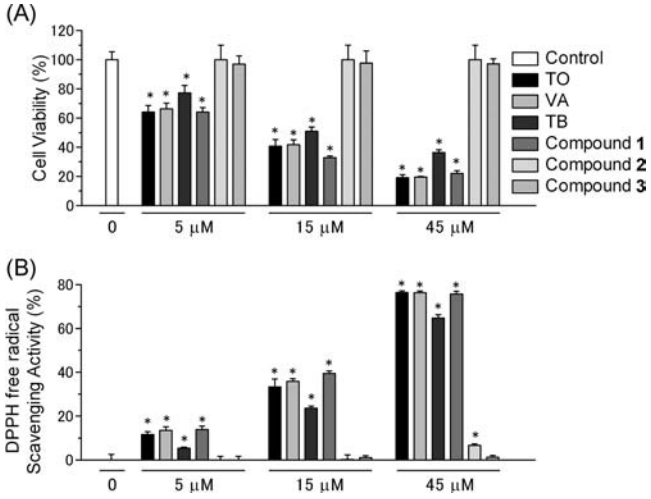

Figure 2. Cytotoxicity against HepG2 cells and DPPH free radical scavenging activity of *p*-terphenyl derivatives. (A) HepG2 cells were treated with various concentrations (5, 15, and 45 μM) of *p*-terphenyl derivatives for 48 h. Cell viability was measured by performing the Neutral Red assay. (B) DPPH radical scavenging activity of various concentrations (5, 15, and 45 μM) of *p*-terphenyl derivatives. Values are expressed as the mean ± SD of three independent experiments. Data were analyzed by ANOVA, followed by Dunnett's test, to compare each group with the control. Differences between the mean values were considered to be significant at (*) $p < 0.01$. TO, thelephantin O; VA, vialinin A; TB, terrestrin B.

Effect of Transition and Alkaline-Earth Metal Ions on TO-Induced Cytotoxicity. Cell viability of HepG2 cells treated with transition and alkaline-earth metal salts for 48 h in the presence or absence of TO (8 μM) was measured. As shown in Figure 3A, 8 μM transition and alkaline-earth metal salts [copper ($CuCl_2$), iron ($FeCl_2$), magnesium ($MgCl_2$), manganese ($MnCl_2$), or zinc ($ZnCl_2$)] did not significantly change cell viability in the absence of TO. However, $FeCl_2$ significantly reversed the TO-induced cytotoxicity in a dose-dependent manner (Figure 3B,C).

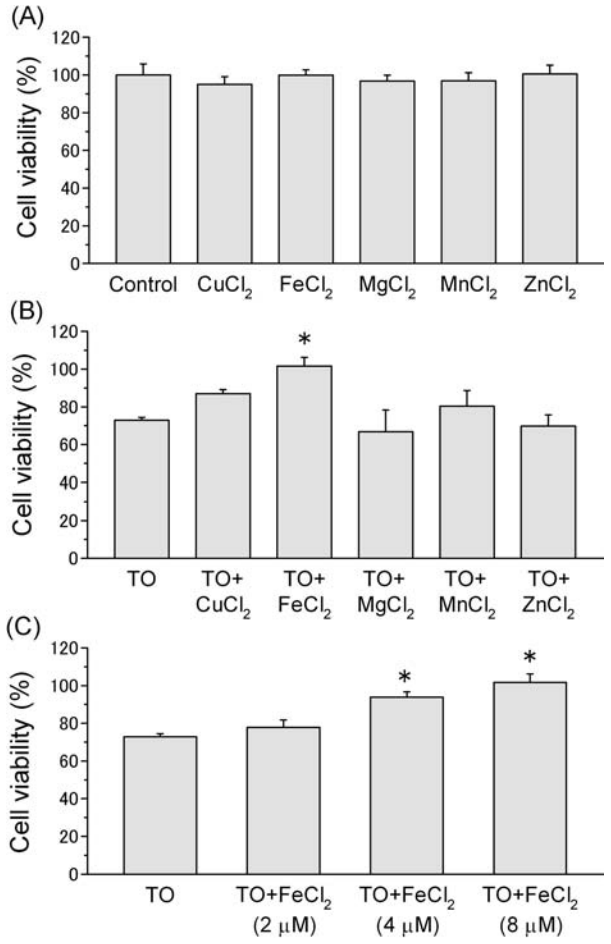

Figure 3. Effect of transition and alkaline-earth metals on cell viability. (A) HepG2 cells were treated with 8 μM transition and alkaline-earth metals for 48 h in the absence of TO. (B) HepG2 cells were treated with 8 μM transition and alkaline-earth metals for 48 h in the presence of 8 μM TO (simultaneous treatment). (C) HepG2 cells were treated with various concentrations of $FeCl_2$ for 48 h in the presence of 8 μM TO (simultaneous treatment). Values are expressed as the mean ± SD of three independent experiments. Data were analyzed by ANOVA, followed by Dunnett's test, to compare each group with (A) the control, (B) TO, and (C) TO. Differences between the mean values were considered to be significant at (*) $p < 0.01$. TO, thelephantin O.

Iron Chelating Activity of *p*-Terphenyl Derivatives. To confirm the affinity of 2′,3′-dihydroxy-*p*-terphenyl derivatives with the iron (Fe^{2+}) ion, we examined the iron (Fe^{2+})-chelating activity of six *p*-terphenyl derivatives with or without a 2′,3′-dihydroxy group (TO, VA, TB, and compounds **1**−**3**). As shown in Figure 4, TO, VA, TB, and compound **1** showed

dx.doi.org/10.1021/jf3041098 | J. Agric. Food Chem. 2013, 61, 1258−1264

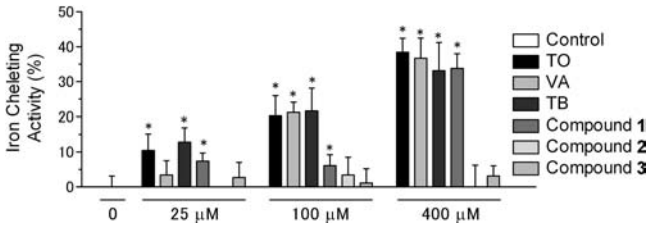

Figure 4. Iron-chelating activity of *p*-terphenyl derivatives. Values are expressed as the mean ± SD of three independent experiments. Data were analyzed by ANOVA, followed by Dunnett's test, to compare with the control. Differences between the mean values were considered to be significant at (*) $p < 0.01$. TO, thelephantin O; VA, vialinin A; TB, terrestrin B.

almost similar iron chelating activities, which followed a dose-dependent pattern; however, compounds **2** and **3** did not show significant chelation for Fe^{2+}, even at a concentration of 400 μM (Figure 4).

Effects of TO and $FeCl_2$ on the Cell Cycle. HepG2 cells were synchronized at the G0/G1 phase of the cell cycle by serum starvation for 36 h (DMEM without serum), followed by stimulation in DMEM supplemented with 10% FBS. HepG2 cells were incubated in 10% FBS-containing DMEM in the absence or presence of 8 μM TO and $FeCl_2$ for 6, 12, or 18 h. As shown in Figure 5, an increase in the S-phase population was detected in the control culture. However, the proportion of cells in the G0/G1 phase increased in the 12 and 18 h treatments in the presence of 8 μM TO, whereas the number of cells in the S phase decreased significantly.

Effects of TO and $FeCl_2$ on the Expression of Genes Related to the Cell Cycle. To examine the molecular mechanism involved in TO-induced cell cycle arrest, the mRNA levels of 84 genes related to cell cycle progression were examined by performing a real-time RT-PCR array. The scatter plots (Figure 6A,B) show a comparison of the gene expression levels between the two experimental conditions. The symbols in the upper left and lower right corner represent up- and down-regulated genes, respectively. Volcano plots (Figure 6C,D) consider statistical significance as well as fold change, organizing genes along dimensions of biological and statistical significance. Each dot in the plot represents a studied gene. As shown in Figure 6A,C, 6 and 13 genes were significantly ($p < 0.01$) up- or

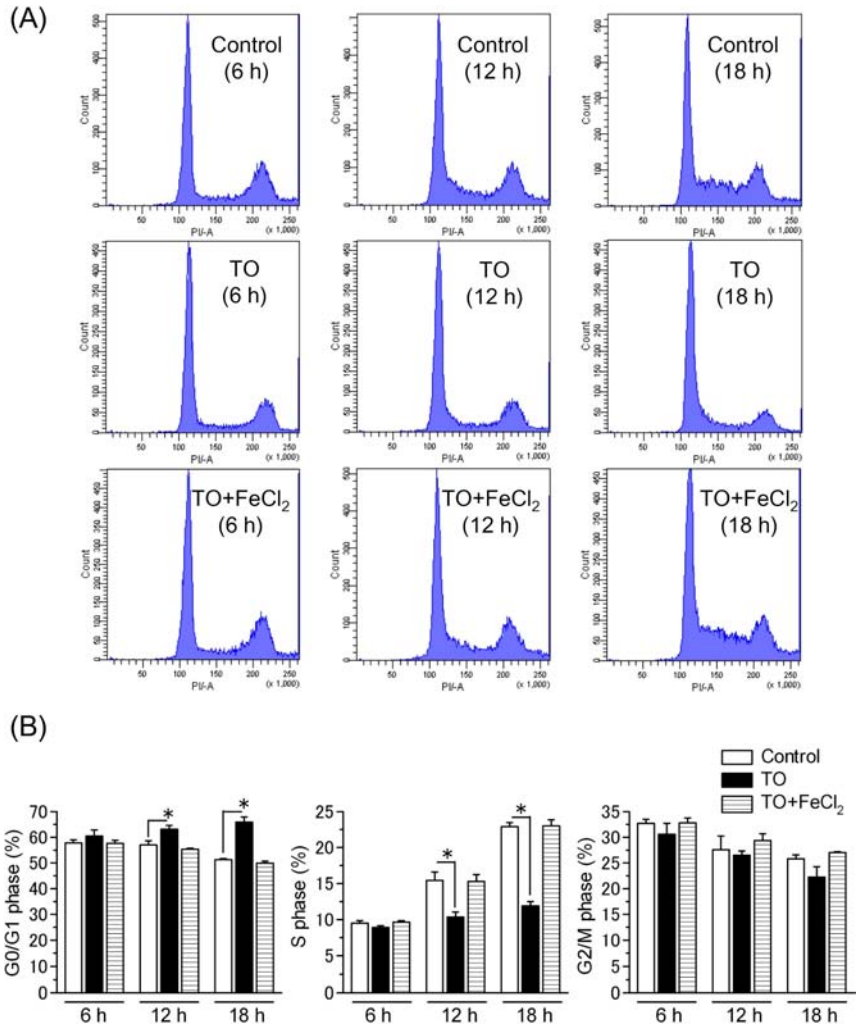

Figure 5. Effects of TO and $FeCl_2$ on the cell cycle. The cell cycle distribution was analyzed by FACSAria using propidium iodide staining of DNA. HepG2 cells were treated with or without 8 μM TO (TO) and $FeCl_2$ for different times. A typical distribution of the DNA content (18 h treatment) and the percentage of cells in each phase of the cell cycle are shown in parts A and B, respectively. Values are expressed as the mean ± SD of three independent experiments. Data were analyzed by ANOVA, followed by Dunnett's test, to compare each group with the control. Differences between the mean values were considered to be significant at (*) $p < 0.01$. TO, thelephantin O.

dx.doi.org/10.1021/jf3041098 | J. Agric. Food Chem. 2013, 61, 1258−1264

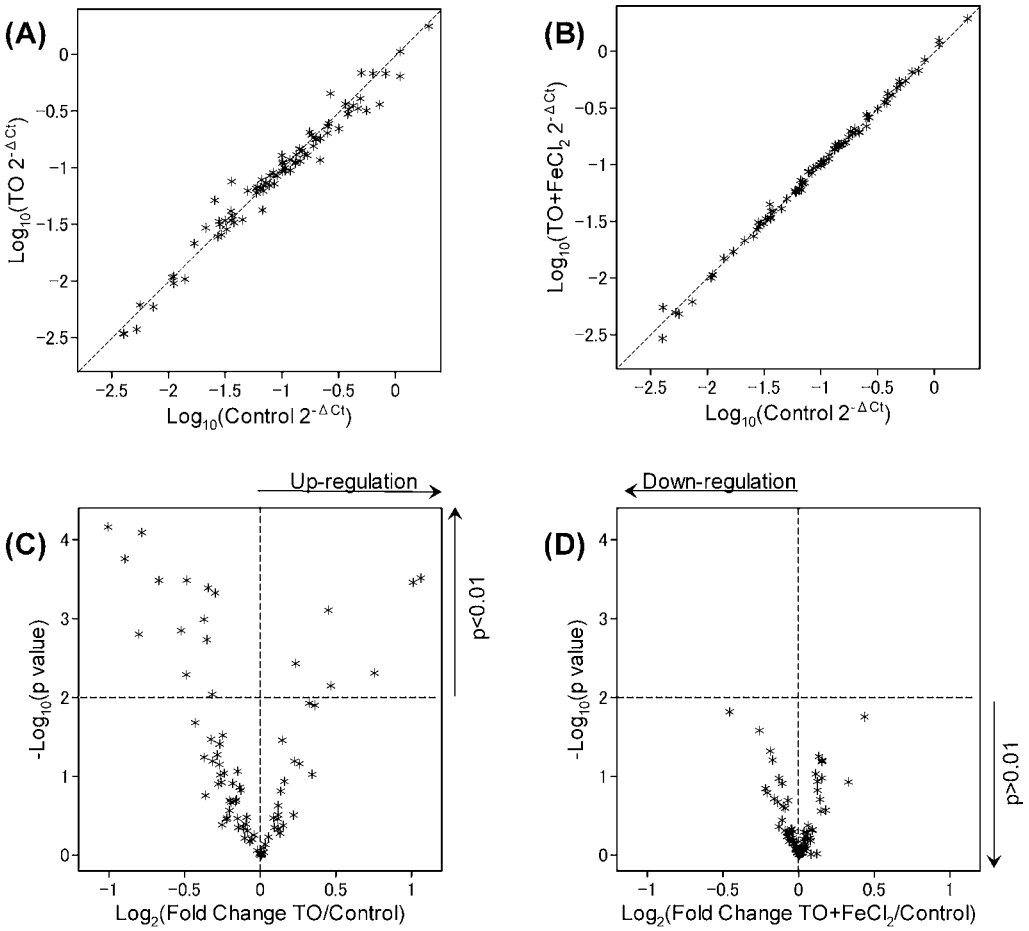

Figure 6. Effects of TO and $FeCl_2$ on the expression of the genes related to the cell cycle. HepG2 cells were treated with or without 8 μM TO (TO) and $FeCl_2$ for 12 h. Values are expressed as the mean ± SD of four independent experiments. The expression of cell cycle-related genes was analyzed by quantitative real-time PCR using the RT2 Profiler PCR Array (Qiagen). The scatter plots express the comparison of gene expression levels between two experimental conditions. The graph plots $\log_{10}$ of normalized gene expression levels in a control (*x*-axis) versus TO [*y*-axis (A)] and TO plus $FeCl_2$ [*y*-axis (B)]. The symbols in the upper left and lower right corner represent the up- and down-regulated genes, respectively. The volcano plots (C, D) indicate the statistical significance of the changes in gene expression. The *x*-axis represents the $\log_2$ of fold change, whereas the *y*-axis represents their *p* value based on Student's *t* test of raw Ct data. TO, thelephantin O.

down-regulated, respectively, by TO treatment. However, the comparison of gene expression profiles between the control versus TO plus $FeCl_2$-treated cells did not display any significant difference ($p > 0.01$) (Figure 6B,D). The fold changes of the mRNA expression levels of these genes are shown in Table 1.

■ DISCUSSION

The major findings of this study were as follows: (i) *o*-dihydroxy substitution of the central benzene ring was necessary for cytotoxicity against HepG2 cells, DPPH free radical scavenging, and iron (Fe^{2+}) chelating activity of *p*-terphenyl derivatives; (ii) the cancer selective cytotoxicity of TO was due to cell cycle arrest at the G1 phase via well-known cell cycle-mediated genes; and (iii) Fe^{2+} chelation occurs in the upstream pathway of TO-induced cell cycle arrest in HepG2 cells.

Terphenyl derivatives are aromatic hydrocarbons consisting of a chain of three benzene rings. Most natural terphenyls are *p*-terphenyl derivatives with poly hydroxyl groups. In vitro, several *p*-terphenyl derivatives have been reported to be as effective as widely used antioxidant agents and immunosuppressive drugs. Recently, during screening for bioactive compounds from *T. aurantiotincta*, we isolated a novel 2′,3′-dihydroxy-*p*-terphenyl derivative, TO, and a related known compound, VA, as selective cytotoxic agents against cancer cells.[4] We have recently reported the chemical synthesis of natural 2′,3′-dihydroxy-*p*-terphenyl derivatives TO, VA, and other 2′,3′-dihydroxy-*p*-terphenyl derivatives, terrestrins B−D, via a practical route and the presence of cytotoxicity against cancer cells in the synthetic compounds.[9] However the mechanism of their bioactivities has not been fully elucidated yet.

In this study, we designed and synthesized three new *p*-terphenyl analogues (compounds **1**−**3**) possessing a VA skeleton bearing partially or fully protected hydroxyl groups, which have not been identified in nature (Supporting Information). To obtain structural information on the biological activities of 2′,3′-dihydroxy-*p*-terphenyl derivatives at the molecular level, six *p*-terphenyl derivatives with or without a 2′,3′-dihydroxy group (TO, VA, TB, and compounds **1**−**3**) were screened for their cytotoxicity against HepG2 cells, as well as for their free radical scavenging activity. Interestingly, TO, VA, TB, and compound **1** showed almost similar cytotoxicities against HepG2 cells and DPPH free radical scavenging activities, which followed a dose-dependent pattern; however, compounds **1** and **2** did not show these activities. These results clearly suggest that the *o*-dihydroxy substitution of the central benzene ring of *p*-terphenyl derivatives is necessary for both the cytotoxicity and antioxidant activities.

Table 1. Fold Change in mRNA Expression of Genes Related to the Human Cell Cycle in HepG2 Cells Treated with Thelephantin O (TO, 8 μM) and $FeCl_2$ (8 μM)

	fold change[a] (% of control)		
gene symbol	control	TO	TO + $FeCl_2$
CCNB1	100 ± 7.4	50.1 ± 7.1*	92.6 ± 3.6
CDKN3	100 ± 8.7	53.9 ± 7.1*	89.7 ± 11.0
CDC20	100 ± 11.1	57.8 ± 10.8*	98.7 ± 9.3
KPNA2	100 ± 8.2	58.1 ± 3.6*	104.4 ± 5.0
CCNF	100 ± 8.9	62.8 ± 4.8*	88.5 ± 4.6
CCNB2	100 ± 6.4	69.9 ± 8.7*	97.5 ± 3.0
CCND2	100 ± 6.1	71.4 ± 4.9*	94.1 ± 7.2
CDK4	100 ± 10.0	71.4 ± 8.9*	101.4 ± 6.4
RAD9A	100 ± 6.6	77.2 ± 3.8*	91.2 ± 10.8
MKI67	100 ± 6.1	78.3 ± 5.5*	98.8 ± 4.2
SKP2	100 ± 5.0	78.7 ± 3.3*	102.4 ± 4.9
CDKN2B	100 ± 10.1	80.0 ± 3.2*	83.4 ± 5.2
CCNC	100 ± 4.3	81.4 ± 3.4*	99.5 ± 7.9
CCNT1	100 ± 5.3	117.6 ± 5.5*	109.7 ± 6.3
CCNG1	100 ± 9.6	136.2 ± 6.4*	101.0 ± 4.7
SERTAD1	100 ± 6.0	138.8 ± 18.5*	99.9 ± 2.6
CDKN1A	100 ± 14.3	169.1 ± 28.5*	96.7 ± 2.4
CCNG2	100 ± 6.6	202.4 ± 27.4*	91.4 ± 6.3
GADD45A	100 ± 24.5	203.7 ± 13.3*	92.5 ± 7.7

[a]Data were analyzed by ANOVA followed by a Dunnett's test to compare each group with the control. Differences between the mean values were considered to be significant at (*) $p < 0.01$.

Previous studies reported that the *o*-dihydroxy structure in naturally occurring polyphenols is necessary for radical stabilization, as well as for metal chelating activity.[10] The close relationship between radical generation and pathogenesis of chronic diseases has been discussed in terms of transition metal homeostasis.[15] In addition, cancer cells are known to require a larger amount of metal ions such as iron, copper, and zinc ions for growth and proliferation than normal cells.[11] Therefore, we hypothesized that the cancer-selective cytotoxicity of 2′,3′-dihydroxy-*p*-terphenyl derivatives TO and VA would result from metal chelation, which would reduce the concentration of the metal ion(s) in cancer cells. To confirm the participation of any metal ions in TO-induced cytotoxicity against HepG2 cells, we measured the cell viability of HepG2 cells treated with several transition and alkaline-earth metal salts ($CuCl_2$, $FeCl_2$, $MgCl_2$, $MnCl_2$, and $ZnCl_2$) for 48 h in the presence or absence of TO (8 μM). These results suggest that each of the metal salts alone induced neither cell proliferation nor cytotoxicity at 8 μM in the absence of TO. However, iron ($FeCl_2$) significantly reversed the TO-induced cytotoxicity in a dose-dependent manner. Thus, it is verified that the Fe^{2+} ion participates in TO-induced cytotoxicity against HepG2 cells. The affinity of 2′,3′-dihydroxy-*p*-terphenyl derivative with the Fe^{2+} ion was also examined by colorimetric analysis using ferrozine. As a result, TO, VA, TB, and compound **1** showed almost similar iron chelating activities, whereas compounds **2** and **3** did not chelate with Fe^{2+}. The correspondence of the structural requirement between the cytotoxicity and Fe^{2+}-chelating ability also supports that the cytotoxicity of 2′,3′-dihydroxy-*p*-terphenyl derivatives against HepG2 cells might be attributable to their iron chelation. We also observed that the DPPH free radical scavenging activity of the 2′,3′-dyhydroxy-*p*-terphenyl derivatives was not suppressed in the presence of $FeCl_2$ even at 45 μM concentration (data not shown). Therefore, the Fe^{2+}-sensitive cytotoxicity of 2′,3′-dyhydroxy-*p*-terphenyl derivatives might not be attributable to their antioxidative activity.

A decrease in cell viability can be the result of either a toxic or a cytostatic effect of 2′,3′-dihydroxy-*p*-terphenyl derivatives. To distinguish between alterations in cell proliferation and cell death, we used cell cycle phase fractionation by flow cytometry, which provides more analytical details of the cell cycle distribution of cell cultures. As shown in Figure 5, the proportion of cells in the G0/G1 phase increased following 12 and 18 h treatments with 8 μM TO, whereas the number of cells in the S phase decreased. In addition, we did not observe sub-G1 DNA fragmentation, a marker of apoptosis, in TO-treated cells. These results suggest that the TO-induced decrease in cell viability was due to cell cycle arrest, but not apoptosis. In addition, TO-induced cell cycle arrest was completely reversed by the addition of $FeCl_2$ (8 μM). The iron ion plays a crucial role in the conversion of ribonucleotides into deoxyribonucleotides by participating in the rate-limiting step of DNA synthesis catalyzed by ribonucleotide reductase.[16] Depletion of iron ion in cells typically results in G1/S arrest, indicating that this metal ion is essential for cell cycle progression.[17] In addition, a previous study reported that plant-derived phenolic compounds showed cytotoxicity against cancer cells via an iron chelation mechanism.[18] These results suggest that iron chelation plays a central role in 2′,3′-dihydroxy-*p*-terphenyl-induced cell cycle arrest.

The mechanisms responsible for G1/S arrest and apoptosis after iron ion depletion have been previously investigated.[19] These studies revealed that a multitude of cell cycle control genes and molecules are regulated by iron ion. As shown in Table 1, 6 and 13 genes were significantly ($p < 0.01$) up- or down-regulated, respectively, by TO treatment. The up-regulated genes, including *CCNG1*,[20] *SERTAD1*,[21] *CDKN1A*,[19] *CCNG2*,[20] and *GADD45A*,[22] and down-regulated genes, including *KPNA2*,[23] *CDK4*,[19] *CCND2*,[19] *MKI67*,[24] *SKP2*,[25] and *CCNC*,[26] were consistent with previously reported changes in gene expression levels associated with cell cycle arrest at the G1/S phase. These results suggest that the growth inhibitory effect of TO was mediated by changes in the expression of these cell cycle-regulated genes. However, comparison of gene expression profiles between the control and TO plus $FeCl_2$-treated cells did not display any significant difference. These results suggest that iron chelation occurred prior to the changes in cell cycle-regulated gene expression in TO-treated HepG2 cells.

In conclusion, the results obtained in the present study demonstrate that the growth inhibitory effect of TO was due to cell cycle arrest at the G1 phase via well-known cell cycle-mediated genes. In addition, TO-induced changes (cell viability, cell cycle, and gene expression) were completely reversed by the addition of $FeCl_2$. These results suggest that iron chelation occurs upstream in the pivotal pathway of TO-induced cell cycle arrest in HepG2 cells. Thus, 2′,3′-dihydroxy-*p*-terphenyl derivatives such as TO and VA were demonstrated to be anticancer agents based on iron chelation. Recently, the iron-chelating activity of flavonoids has been studied, and their structure–activity relationships have been presented.[27] However, this is the first study to show the association of the iron-chelating activity of 2′,3′-dihydroxy-*p*-terphenyl derivatives with their cytotoxicity against cancer cells. Further in vivo biological studies on 2′,3′-dihydroxy-*p*-terphenyl derivatives are underway.

■ ASSOCIATED CONTENT

Supporting Information

Synthetic preparation of compounds **1**−**3**. This material is available free of charge via the Internet at http://pubs.acs.org.

■ AUTHOR INFORMATION

Corresponding Author

*Phone/fax: +81 17 765 4214. E-mail: t_norikura@auhw.ac.jp.

Funding

This work was supported by grants from the Designated Research Fund for Academic Research at Aomori University of Health and Welfare.

Notes

The authors declare no competing financial interest.

■ ABBREVIATIONS USED

TO, thelephantin O; VA, vialinin A; TB, terrestrin B

■ REFERENCES

(1) Newman, D. J.; Cragg, G. M.; Snader, K. M. Natural products as sources of new drugs over the period 1981−2002. *J. Nat. Prod.* **2003**, *66*, 1022−1037.

(2) Quang, D. N.; Hashimoto, T.; Asakawa, Y. Inedible mushrooms: a good source of biologically active substances. *Chem. Rec.* **2006**, *6*, 79−99.

(3) Lin, H.; Ji-Kai, L. *p*-Terphenyls from the basidiomycete *Thelephora aurantiotincta*. *Z. Naturforsch.* **2003**, *58*, 452−454.

(4) Norikura, T.; Fujiwara, K.; Narita, T.; Yamaguchi, S.; Morinaga, Y.; Iwai, K.; Matsue, H. Anticancer activities of thelephantin O and vialinin A isolated from *Thelephora aurantiotincta*. *J. Agric. Food Chem.* **2011**, *59*, 6974−6979.

(5) Xie, C.; Koshino, H.; Esumi, Y.; Takahashi, S.; Yoshikawa, K.; Abe, N. Vialinin A, a novel 2,2-diphenyl-1-picrylhydrazyl (DPPH) radical scavenger from an edible mushroom in China. *Biosci., Biotechnol., Biochem.* **2005**, *69*, 2326−2332.

(6) Onose, J.; Xie, C.; Ye, Y. Q.; Sugaya, K.; Takahashi, S.; Koshino, H.; Yasunaga, K.; Abe, N.; Yoshikawa, K. Vialinin A, a novel potent inhibitor of TNF-α production from RBL-2H3 cells. *Biol. Pharm. Bull.* **2008**, *31*, 831−833.

(7) Ye, Y. Q.; Koshino, H.; Onose, J.; Yoshikawa, K.; Abe, N.; Takahashi, S. Studies on natural *p*-terphenyls: total syntheses of vialinin A and terrestrin B. *Biosci., Biotechnol., Biochem.* **2010**, *74*, 140−146.

(8) Ye, Y. Q.; Koshino, H.; Onose, J.; Negishi, C.; Yoshikawa, K.; Abe, N.; Takahashi, S. Structural revision of thelephantin G by total synthesis and the inhibitory activity against TNF-α production. *J. Org. Chem.* **2009**, *74*, 4642−4645.

(9) Fujiwara, K.; Sato, T.; Sano, Y.; Norikura, T.; Katoono, R.; Suzuki, T.; Matsue, H. Total synthesis of thelephantin O, vialinin A/terrestrin A, and terrestrins B−D. *J. Org. Chem.* **2012**, *77*, 5161−5166.

(10) Nagy, M.; Krizkova, L.; Mucaji, P.; Kontsekova, Z.; Sersen, F.; Krajcovic, J. Antimutagenic activity and radical scavenging activity of water infusions and phenolics from ligustrum plants leaves. *Molecules* **2009**, *14*, 509−518.

(11) Kalinowski, D. S.; Richardson, D. R. The evolution of iron chelators for the treatment of iron overload disease and cancer. *Pharmacol. Rev.* **2005**, *57*, 547−583.

(12) Liu, J. K.; Hu, L.; Dong, Z. J.; Hu, Q. DPPH radical scavenging activity of ten natural *p*-terphenyl derivatives obtained from three edible mushrooms indigenous to China. *Chem. Biodivers.* **2004**, *1*, 601−605.

(13) Zhang, S. Z.; Lipsky, M. M.; Trump, B. F.; Hsu, I. C. Neutral red (NR) assay for cell viability and xenobiotic-induced cytotoxicity in primary cultures of human and rat hepatocytes. *Cell Biol. Toxicol.* **1990**, *6*, 219−234.

(14) Kim, E. Y.; Ham, S. K.; Shigenaga, M. K.; Han, O. Bioactive dietary polyphenolic compounds reduce nonheme iron transport across human intestinal cell monolayers. *J. Nutr.* **2008**, *138*, 1647−1651.

(15) Lipinski, B. Hydroxyl radical and its scavengers in health and disease. *Oxid. Med. Cell. Longev.* **2011**, *2011*, 809696.

(16) Nyholm, S.; Mann, G. J.; Johansson, A. G.; Bergeron, R. J.; Graslund, A.; Thelander, L. Role of ribonucleotide reductase in inhibition of mammalian cell growth by potent iron chelators. *J. Biol. Chem.* **1993**, *268*, 26200−26205.

(17) Le, N. T.; Richardson, D. R. The role of iron in cell cycle progression and the proliferation of neoplastic cells. *Biochim. Biophys. Acta* **2002**, *1603*, 31−46.

(18) Sestili, P.; Diamantini, G.; Bedini, A.; Cerioni, L.; Tommasini, I.; Tarzia, G.; Cantoni, O. Plant-derived phenolic compounds prevent the DNA single-strand breakage and cytotoxicity induced by *tert*-butylhydroperoxide via an iron-chelating mechanism. *Biochem. J.* **2002**, *364*, 121−128.

(19) Yu, Y.; Kovacevic, Z.; Richardson, D. R. Tuning cell cycle regulation with an iron key. *Cell Cycle* **2007**, *6*, 1982−1994.

(20) Faradji, F.; Bloyer, S.; Dardalhon-Cumenal, D.; Randsholt, N. B.; Peronnet, F. *Drosophila melanogaster* cyclin G coordinates cell growth and cell proliferation. *Cell Cycle* **2011**, *10*, 805−818.

(21) Watanabe-Fukunaga, R.; Iida, S.; Shimizu, Y.; Nagata, S.; Fukunaga, R. SEI family of nuclear factors regulates p53-dependent transcriptional activation. *Genes Cells* **2005**, *10*, 851−860.

(22) Satomi, Y.; Nishino, H. Implication of mitogen-activated protein kinase in the induction of G1 cell cycle arrest and gadd45 expression by the carotenoid fucoxanthin in human cancer cells. *Biochim. Biophys. Acta* **2009**, *1790*, 260−266.

(23) Hawkes, W. C.; Wang, T. T.; Alkan, Z.; Richter, B. D.; Dawson, K. Selenoprotein W modulates control of cell cycle entry. *Biol. Trace Elem. Res.* **2009**, *131*, 229−244.

(24) Scholzen, T.; Gerdes, J. The Ki-67 protein: from the known and the unknown. *J. Cell. Physiol.* **2000**, *182*, 311−322.

(25) Sumimoto, H.; Hirata, K.; Yamagata, S.; Miyoshi, H.; Miyagishi, M.; Taira, K.; Kawakami, Y. Effective inhibition of cell growth and invasion of melanoma by combined suppression of BRAF (V599E) and Skp2 with lentiviral RNAi. *Int. J. Cancer* **2006**, *118*, 472−476.

(26) Ren, S.; Rollins, B. J. Cyclin C/cdk3 promotes Rb-dependent G0 exit. *Cell* **2004**, *117*, 239−251.

(27) Mladenka, P.; Macakova, K.; Filipsky, T.; Zatloukalova, L.; Jahodar, L.; Bovicelli, P.; Silvestri, I. P.; Hrdina, R.; Saso, L. In vitro analysis of iron chelating activity of flavonoids. *J. Inorg. Biochem.* **2011**, *105*, 693−701.